

Scientific paper

# An Expanded EXAFS Model of Mn, Zn, and Fe Spinel Nanoparticles

Alojz Kodre<sup>1,3\*</sup>, Iztok Arčon<sup>2,3</sup>, Jana Padežnik Gomilšek<sup>4</sup>, Darko Makovec<sup>3</sup><sup>1</sup> Faculty of Mathematics and Physics, Jadranska 19, SI-1000 Ljubljana, Slovenia<sup>2</sup> University of Nova Gorica, Vipavska 13, SI-5000 Nova Gorica, Slovenia<sup>3</sup> Jožef Stefan Institute, Jamova 39, SI-1000 Ljubljana, Slovenia<sup>4</sup> Faculty for Mechanical Engineering, Smetanova 17, SI-2000 Maribor, Slovenia\* Corresponding author: E-mail: [alozj.kodre@mf.uni-lj.si](mailto:alozj.kodre@mf.uni-lj.si)

Received: 18-06-2007

## Abstract

The structure of Mn, Zn, Fe spinel nanoparticles, obtained by coprecipitation from reversed microemulsions, deviates progressively with the diminishing particle size from the bulk spinel structure. The deviations can in principle be extracted from EXAFS spectra of constituent metals, but with additional parameters to describe the deviations, the problem may not remain statistically well-posed. With a simultaneous analysis of the spectra, enabled by the recently available IFEFFIT code, the well-posedness is regained, and several types of deviations, introduced by nanoscopic size or by varied stoichiometry of oxide mixtures can be quantified: the changes in site occupations, the distortion of the lattice and the fraction of vacancies.

**Keywords:** (Mn, Zn) ferrites, spinel nanoparticles, EXAFS analysis, multiple EXAFS spectra fitting.

## 1. Introduction

The manganese-zinc ferrite nanoparticles synthesized with coprecipitation from reversed microemulsions are characterized by a rather narrow size distribution with size depending on the parameters of the preparation.<sup>1</sup> Although the corresponding bulk material crystallizes in a well-defined spinel lattice, the coprecipitation yields a non-equilibrium product where the spinel unit cell may be modified to a considerable extent. In addition to that, the nanoscopic nature of the grains introduces further modifications: the large percentage of the surface atoms means a noticeable average deficit in the coordination numbers, and a change in the average bond length.

The spinel structure, characterized by the net formula  $AB_2O_4$ , is by itself highly flexible, the normal occupation of tetrahedral A sites with a divalent metal, and of octahedral B sites with a trivalent metal, can be, depending on the ionic radii of the constituents, modified by site-swapping all the way to the inverse spinel. Crystallographically, the apparent richness of structure is still described within the same space group,  $Fd\bar{3}m$ , quantified by just

two parameters, the size of the unit cell, and the »oxygen parameter«, accounting for the possible tilt of the oxygen polyhedra and not affecting the positions of the metal ions.

XRD (X-Ray Diffraction) is the method of choice for determination of these two basic parameters; further structure characteristics, such as site occupation probabilities, are accessible only indirectly, through the refinement techniques whereby positions of atoms in the unit cell are adjusted by a best fit to the data.

EXAFS (Extended X-ray Absorption Fine Structure) offers a direct way to measure the parameters of an atom neighborhood: the average distance to neighbors of a given species, their number and the width of their radial distribution. Calvin et al.<sup>2</sup> have shown how the site occupation can be deduced in a least-square relaxation, implemented in the IFEFFIT code,<sup>3,4</sup> of a model of the unit cell. In the present study, we extend the technique to the determination of additional structural properties: the distortion of the structure in nanoscopic particles and their adaptation to improper stoichiometry with enhanced site-swapping or creation of vacancies.

The extension of the parameter space is only possible with a simultaneous relaxation of the model EXAFS spectra of the constituent metals with the measured data. General advantages of simultaneous EXAFS analysis are discussed in Conclusions.

## 2. Experimental

Two series of spinels in the (MnO–ZnO–Fe<sub>2</sub>O<sub>3</sub>) system were prepared:

- Manganese-zinc ferrite nanopowders (Mn:Zn:Fe =1:1:4) with average particle diameters of 7 nm, 4.5 nm, 3 nm, 2 nm and 1.5 nm (MZF-7 to MZF-1.5) were synthesized using co-precipitation in reverse microemulsions;<sup>1</sup>
- Mn/Zn quasispinels with Mn:Zn ratio of 4:5 and 2:1 and particle size above 50 nm (MZ-4/5 and MZ-2/1) were synthesized via oxalate precursors.<sup>5</sup>

The average particle sizes were estimated from the XRD peak broadening using Debye-Scherrer method.

Samples for x-ray absorption spectroscopy were prepared from the powders in the form of tablets of optimum thickness ( $\mu\text{d} \sim 2$ ) with boron nitride matrix. Powdered (Mn,Zn)Fe<sub>2</sub>O<sub>4</sub> ceramics, synthesised by sintering and regrinding of the oxide mixture, was used as a standard, prepared in the same form.

EXAFS spectra at the K edges of the constituent metals were measured at room temperature in a standard transmission detection mode on the x-ray absorption beamlines E4 and C of HASYLAB, DESY (Hamburg). Si(111) double crystal monochromators with energy resolution  $\sim 1$  eV were used. The rejection of the beam harmonics was implemented with a flat Au mirror and with dynamic detuning of the crystals to the 60% of the rocking-curve maximum. The absorption spectra were measured within the interval  $[-250 \text{ eV} \dots 1000 \text{ eV}]$  relative to the respective K edge, except for Mn where the spectrum is truncated to 570 eV by the subsequent Fe K edge. The EXAFS region is scanned with equidistant k-step of  $\sim 0.03 \text{ \AA}^{-1}$  and integration time of 2 s/step. Several consecutive runs of each spectrum are superposed to improve the signal-to-noise ratio. Precise energy calibration of the spectra was ensured by a simultaneous absorption measurement on corresponding metal foils.

## 3. Results and Discussion

The measured spectra are processed for analysis with the IFEFFIT code Athena.<sup>4</sup> The richest example, the triplets of spectra of (Mn,Zn) ferrite nanoparticles (MZF-n), is presented in the standard way – absolute value of the Fourier transform (FT) – which offers some direct visualization (Fig. 1).

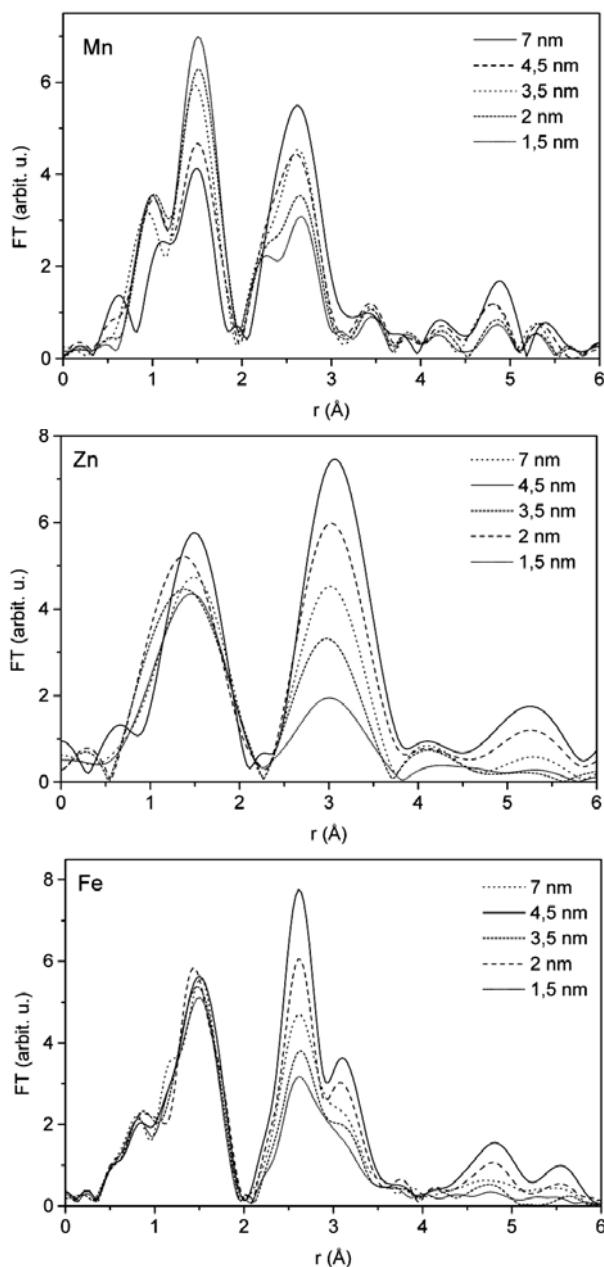


**Figure 1.** Fourier-transformed  $k^3$ -weighted EXAFS spectra of Mn, Zn and Fe in the MZF-n nanoparticles. The amplitudes diminish monotonously with particle size n.

The data can be most easily interpreted in a comparison with some standard structure. EXAFS spectra of the same compound, prepared as a ceramic polycrystallite, are shown in a common plot (Fig. 2).

FT EXAFS can be regarded as an (approximate) radial distribution of the neighbors. All three metals have the first neighbors (oxygen atoms) at about the same distance, as suggested by the first peak in the three spectra at around 1.7 Å, taking into account that peaks in the EXAFS FT spectra are systematically shifted to lower r values – in this case for about 0.3 Å.

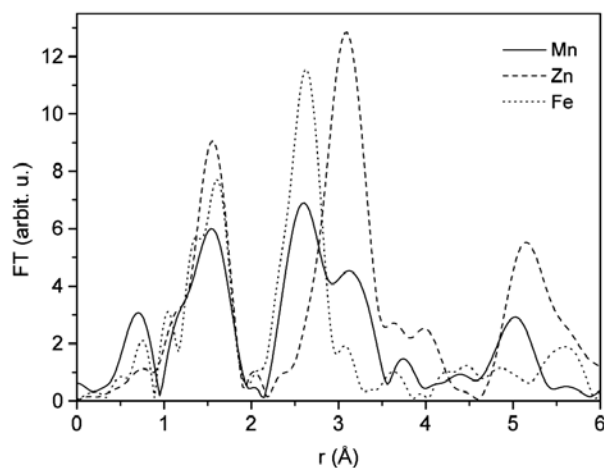


**Figure 2.** Fourier-transformed  $k^3$ -weighted EXAFS spectra of the (Mn,Zn) ferrite ceramics from the  $k$ -range of  $3.5\text{--}12\text{ \AA}^{-1}$ . The data of the three metals are shown in a common plot to emphasize common features and differences in their neighborhoods.

The second neighbors in the spinel lattice are metal atoms. Zn atom, occupying predominantly A (tetrahedral) sites, has second neighbors from  $3.5\text{ \AA}$  on, and Fe, mainly on B (octahedral sites), from  $3\text{ \AA}$  on. Mn occupation, apparently, is divided between the two sites, having second neighbors at both distances.

The neighborhoods of MZF- $n$  follow basically the same scheme as the standard above. In Mn, however, the second-neighbor peak shows hardly any amplitude beyond  $3\text{ \AA}$ , where the A-site second-neighbor shell should appear. Even more, there is a component of the peak at the proper distance of  $2.5\text{ \AA}$ , which is far below the shortest second-neighbor distance of  $3\text{ \AA}$  in spinels.

The FT spectra of MZF- $n$  are quite informative on the effect of the grain size. All amplitudes change monotonously with grain size. In Zn and Fe, the amplitude of first-neighbor peak is steady, pointing to a steady (and complete) occupation of the oxygen polyhedra. The systematic increase in Mn can be explained with site swapping, the exchange from tetrahedral to octahedral oxygen mantle in ever smaller grains.

The number of second neighbors decreases with grain size for all metals. The relative rate of the decrease is comparable in Fe and Mn, and somewhat stronger in Zn, judging from the ratio of the smallest to the largest peak. The effect is explained by the truncated neighborhood of the surface atoms, which prevail with the decrease of the grain size.<sup>6</sup>

#### 4. Quantitative Models

In the above simplified discussion, the structural information of the EXAFS FT spectra up to  $\sim 4\text{ \AA}$  was explained as a superposition of merely three neighbor shells: oxygen atoms in the first shell, and the metal atoms in the

second shell, different for sites A and B. In the theory of EXAFS, the measured signal is expanded into a sum of contributions from possible scattering paths of the photoelectron. The paths are ordered by the increasing length and scattering order. Only the shortest single-scattering paths correspond to the neighbor shells in the simplified picture, their lengths separated sufficiently to produce individual peaks of the radial density. In spinels, e.g., the contact distance Me–O is close to  $2\text{ \AA}$ , and the distance to the closest metal neighbor is larger by a factor of  $\sqrt{3}$  or  $\sqrt{2}$ , for the sites A and B, respectively. The distribution of distances to further neighbors becomes steadily denser, especially when the multiple-scattering paths are included. The effect is shown in Fig. 3, where the contributions of individual scattering paths up to  $3.7\text{ \AA}$  are shown for the Fe EXAFS of the ceramic standard.

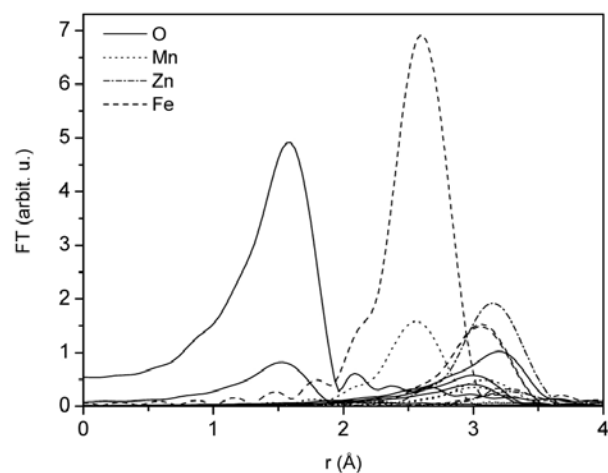


**Figure 3.** Theoretical contributions of the first 17 single-scattering paths up to the length of  $3.7\text{ \AA}$  to the Fe EXAFS in the ceramic (Mn, Zn) ferrite standard in Fig. 2.

It is evident hence that EXAFS analysis is limited to a few closest neighbors, for which the number of path contributions, and the number of parameters for their description, remains manageable. The equivalent of our qualitative simplified picture is an *ad-hoc* model in which the tentative first – and possibly second – neighbor atoms are placed at estimated distances without any crystallographic order, or indeed, without any spatial relation between them. The artificial EXAFS signal, calculated from this placement of atoms, is then relaxed by variation of the model distances for the best match with the measured data. Alongside, the multiplicity of the neighbors and the widths of their radial distribution are obtained by a similar process of repeated small variations, by which the model spectrum is fitted to the experimental spectrum. The approach is useful when little or no *a priori* information on the structure is available, as e.g. in disordered materials.

In our case, the general crystallographic structure of the materials is well-known, so that ideal spatial positions

of the neighbors can be inserted into the model. Indeed, the entire range of true positions can be expressed just by two parameters, the isotropic expansion factor to adjust the tabulated unit-cell size to the investigated sample, and the oxygen parameter. Further parameters are required to describe the metal/site occupation probabilities and the widths of the radial distribution of individual neighbors.

#### 4. 1. Mn-Zn Ferrite

In their study, Calvin *et al.*<sup>2</sup> built a very economical model with just 16 parameters: the 6 occupation probabilities are all expressed by only 2 independent parameters, and

the widths (Debye-Waller factors) are constrained to a common value for entire groups of neighbors. Even with this economy, the information content of individual EXAFS spectrum is not sufficient to yield statistically meaningful values to the parameters in the least-square relaxation. The EXAFS signals of all three metals together, however, with the information content tripled, provide a satisfactory basis for determination of the parameters. There is another crucial gain in the simultaneous relaxation: the values of the parameters are already optimized for the three spectra. The mirror relations, the requirements that the length and width of a scattering path included in two EXAFS must be the same from either end, are automatically satisfied.

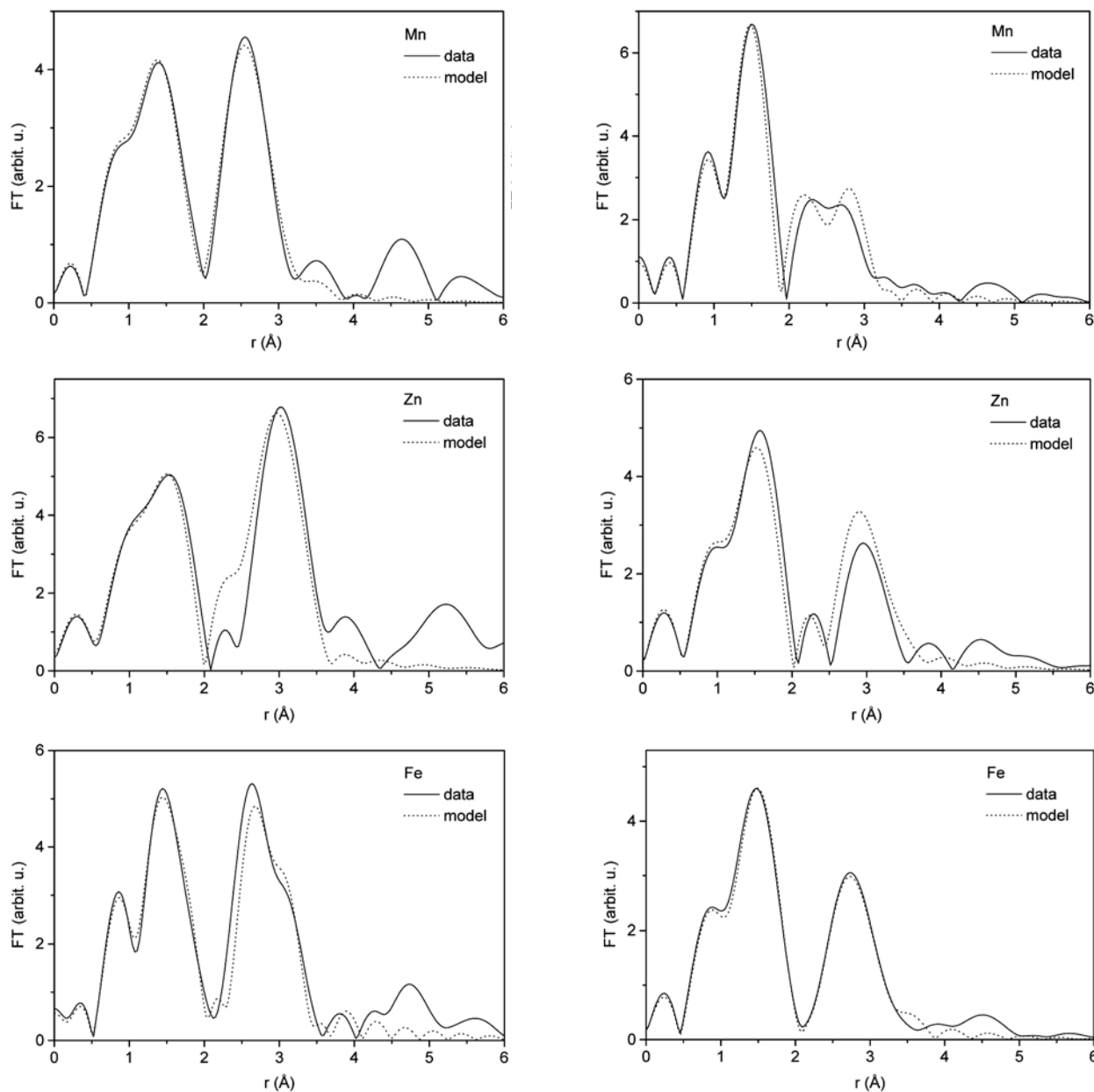


**Figure 4.** FT magnitude of the  $k^3$ -weighted Mn, Zn and Fe EXAFS with the improved model for the standard (left) and the worst case MZF-1.5 (right).

Calvin *et al* studied the site-occupation probabilities in coprecipitated spinels of a fixed stoichiometry, depending on the synthesis parameters. The spinel particles had typical diameters of a few tens of nm, so that their structure departed only negligibly from the bulk structure.

In our case, the conditions of the synthesis were adjusted for production of nanoparticles with much smaller average grain sizes, from 10 down to 1.5 nm. The EXAFS model, based on the published data on the ceramic standard<sup>7</sup> of the same stoichiometry, akin to the model of Calvin *et al*, yielded extremely poor results. It could be relaxed to fit the EXAFS signal of the ceramic standard sample quite satisfactorily, but the fits to the MZF-n samples, as judged by the quality-of-fit measure, were at least 10 times worse. Apparently, the model could not be adjusted to the specific features of the nanoparticles.

As a remedy, additional parameters were introduced:

- the effective second-neighbor occupation, a parameter in the range [0, 1], to describe the deficiency in the metal-metal correlation for the atoms at the surface;
- the site-dependent and ion-dependent corrections to the metal-metal distances. The former are used to describe additional distortions of the spinel lattice near the surface, and the latter to describe the di-

stortions due to different ion sizes. In each group, the corrections are constrained to zero sum, so that they introduce no net expansion of the lattice.

The fits are essentially improved, with the quality-of-fit measure within a factor of 2 of the standard (Fig 4).

## 4. 2. Zn-Mn Spinel

Single-phase Zn-Mn spinels synthesized via oxalate precursors were obtained for Mn:Zn atomic ratios of 2:1 and 4:5. The initial attempt to fit their EXAFS spectra with the standard spinel model produced unusual results.

Apparently, one of the metals is well described by our "universal" spinel model, the other poorly. The "good" metal is Zn in MZ-2/1, and Mn in MZ-4/5; in both cases, the fit is perfect. For the "bad" metal, evidently, the model misses something essential. So, further adaptations of our model, successfully employed in Mn-Zn ferrites, are required.

A double oxide with the Mn:Zn = 4:5 ratio has recently been reported.<sup>8</sup> The ratio is quite far from the normal spinel value, and mere swapping of sites evidently cannot accommodate the stoichiometry. Further adaptation of the structure is possible through vacancies: accordingly, the model is expanded with vacancy parameters.

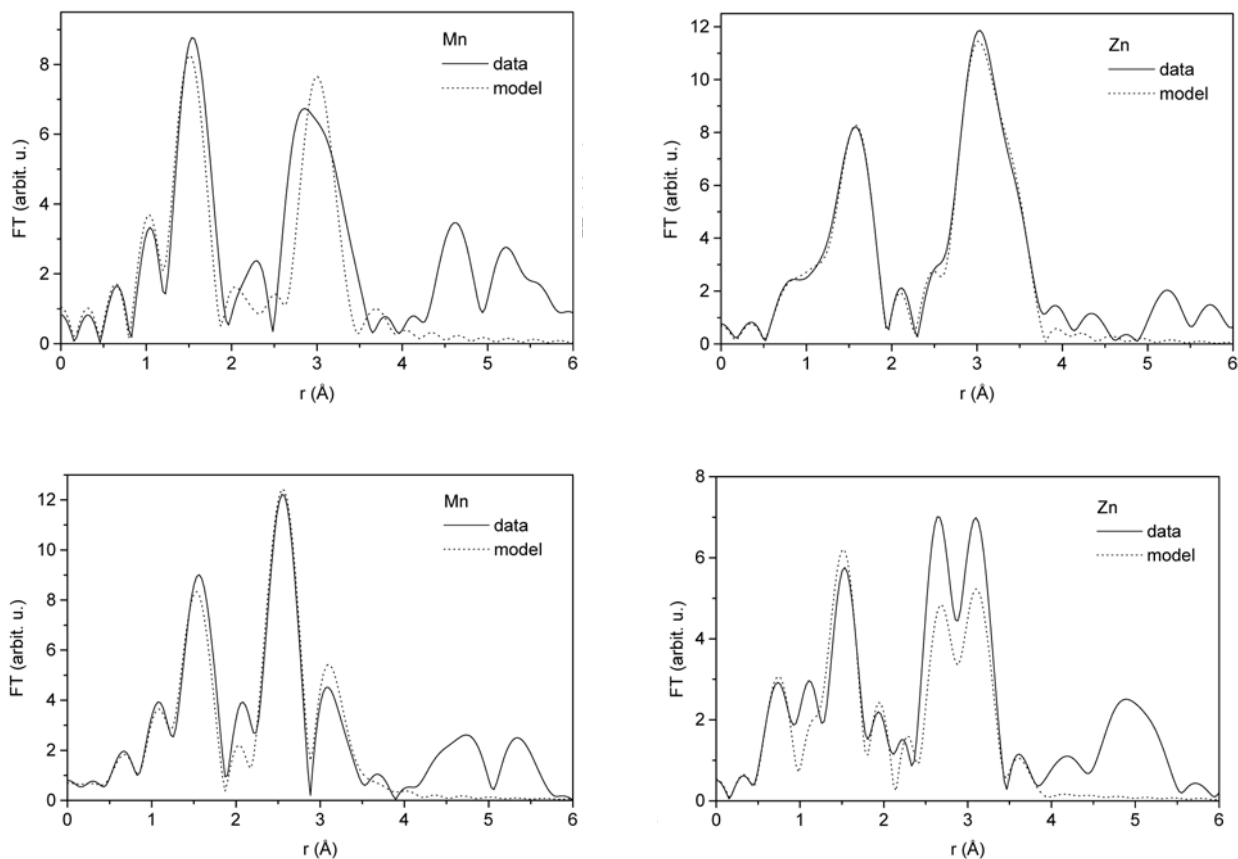


**Figure 5.** FT magnitude of the  $k^3$ -weighted Mn (left) and Zn (right) EXAFS FT of MZ-2/1 (above) and MZ-4/5 (below) together with the conventional spinel model.

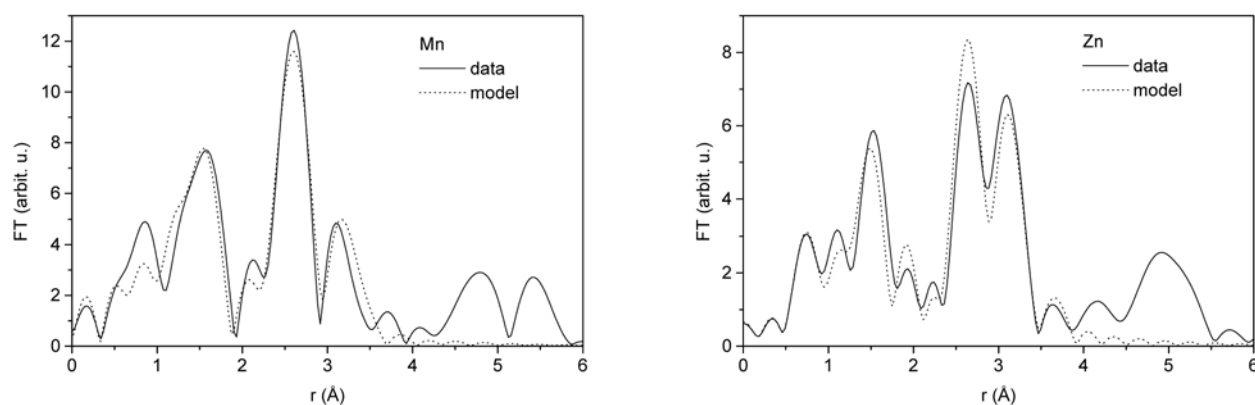


Figure 6. FT magnitude of the  $k^3$ -weighted Mn and Zn EXAFS with the improved model for the MZ-4/5.

The quality of the fit is improved to better than 6% (Fig. 6). The results suggest 8% of vacant B sites and 29% of A sites. The swapping of sites relieves the large excess of Zn: about 40% of the metal resides on B sites, while no Mn moves to A sites.

For the MZ-2/1 spinel, the extra width of the second-neighbor peak is a hint of a split neighbor shell, for instance due to the Jahn-Teller effect in Mn octahedra, leading to a tetragonal distortion of the lattice. (A tetragonal double oxide ceramics with the same stoichiometry is reported in the ICSD base.<sup>9</sup>) To allow for the distortion, the Mn–O and Mn–Mn scattering paths are cloned with a small length difference, the intensities divided in the ratio 2 : 4. The fit is immediately improved, the obtained splitting is 0.21 Å for Mn–Mn and 0.33 Å for Mn–O. (For the tetragonal ceramics, the values of 0.21 Å and 0.28 Å, respectively, can be deduced from crystallographic data.)

Vacancy parameters are also included in the model. Separate values for A and B sites make the fit unstable. A single parameter for the average vacancy probability, however, gives a stable value of  $(29 \pm 7) \%$ . The swapping of sites in this material is almost nonexistent. Mn occupies B sites, moving to A sites in less than 6%. Zn occupies only A sites. The quality of fit is 1.5% (Fig. 7).

## 5. Conclusions

The spinel crystal lattice, by itself quite variable with regard to site occupation, can be further modified to include slight deviations introduced by the micellar coprecipitation in which the relaxation of the structure is very weak due to the low temperature of the process, and by the frustrated site occupation in the mixed Mn/Zn oxide. For the two cases, different adaptation tools were introduced: reduction in coordination and adjustments of the bond lengths for nanoscopic particles, and vacancy probability with splitting of bond lengths for Zn–Mn quasispines.

In EXAFS analysis, the tools are extensions of the parameter space: to ensure the statistical definiteness of the model, the data space has to be expanded accordingly. This is most readily achieved by a simultaneous fitting of several EXAFS spectra. An additional advantage is the automatic fulfillment of mirror relations between scattering-path parameters.

Simultaneous fitting is statistically sound in any case of parameter coupling. In the present study where the same structure is examined through EXAFS signals of three constituent elements, its application is most straight-

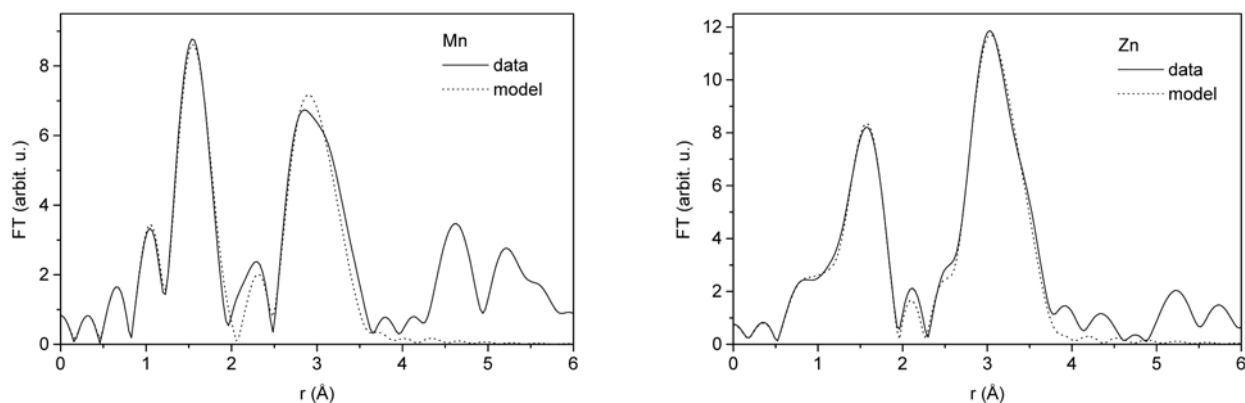


Figure 7. FT magnitude of the  $k^3$ -weighted Mn and Zn EXAFS with the improved model for the MZ-2/1.

forward. Another plain case is the study of a material at different temperatures. More generally, however, EXAFS studies seldom involve a single spectrum: usually, a series of related samples is analyzed. Simultaneous fitting is warranted by the presence of common or related parameters in the series. The sound practice of EXAFS analysis with standards is a particularly widespread case.

The implementation of simultaneous fitting is limited only by computer speed and memory requirements. Undoubtedly, the processing time grows faster than linearly with the number of spectra. However, simultaneous fitting is always faster than consecutive single-spectrum fitting, where the same degree of inter-parameter consistency is obtained only after many iterations of the series.

Currently, the IFEFFIT package<sup>4</sup> enables simultaneous fitting of four EXAFS spectra with typically 100 parameters. It has opened up the way to solve the problems, such as the above, which are effectively intractable with single-spectrum fitting. However, the simultaneous analysis of series of EXAFS data could require a space larger for an order of magnitude. With the massive production of EXAFS data as envisioned for the x-ray sources of the next generation, as e.g. free-electron x-ray lasers, the need for simultaneous analysis will undoubtedly explode.

## 6. Acknowledgments

This work was supported by the Slovenian Research Agency research programme P1-0112, by DESY, the European Community under the FP6 Programme “Structuring the European Research Area” contract RII3-CT-2004-506008 (IA-SFS). Access to synchrotron radiation facilities of HASYLAB (beamline E4, project II-04-065) is acknowledged. We would like to thank Edmund Welter of HASYLAB for expert advice on beamline operation.

## Povzetek

Struktura nanodelcev (Mn, Zn, Fe)-spinela, ki nastanejo s ko-obarjanjem v reverzni mikroemulziji, se z vse manjšim premerom zrn vse bolj oddaljuje od strukture spinela. Odstopanja načeloma lahko razberemo iz spektrov EXAFS vseh treh kovin, vendar se z naraščajočim številom parametrov, ki so potrebni za opis odstopanj, zmanjšuje statistična pogojenost problema. S hkratno analizo vseh treh spektrov, kot jo omogoča najnovejši program IFEFFIT, ohranimo statistično pogojenost in tako lahko ovrednotimo različne tipe strukturnih odstopanj: spremembe v zasedbeni porazdelitvi po kristalnih mestih, distorzijo mreže in delež vrzeli v zasedbi.

## 7. References

1. D. Makovec, A. Košak, M. Drogenik, *Nanotechnology* **2004**, *15*, S160–S166.
2. S. Calvin, E. E. Carpenter, B. Ravel, V. G. Harris, S. A. Morrison, *Phys. Rev. B* **2002**, *66*, 224405.
3. J. J. Rehr, J. M. de Leon, S. I. Zabinsky, R. C. Albers, *J. Am. Chem. Soc.* **1991**, *113*, 5135–5140.
4. B. Ravel, M. Newville, *J. Synchrotron Rad.* **2005**, *12*, 537–541.
5. M. Peiteado, A. C. Caballero, D. Makovec, *J. Europ. Ceram. Soc.* **2007**, *27*, 3915–3918.
6. I. Arson, A. Tuel, A. Kodre, G. Martin, A. J. Barbier, *J. Synchrotron Rad.* **2001**, *8*, 575–577
7. U. Koenig, G. Chol, *J. Appl. Cryst.* **1968**, *1*, 124–126.
8. J. Blasco, J. Garcia, *J. Sol. State. Chem.* **2006**, *179*, 2199–2205.
9. M. Nogues, P. Poix, *JPCSA* **1962**, *23*, 711–727.